

## Imaging atoms in the field-ion microscope: Tunneling calculations using realistic potentials

S. C. Lam and R. J. Needs

*Cavendish Laboratory, University of Cambridge, Cambridge CB3 0HE, United Kingdom*

(Received 20 July 1993)

A self-consistent pseudopotential technique is used to calculate the electron potential for adatom, stepped, and atomically smooth Al (111) surfaces with a perpendicular applied electric field of  $3 \text{ V \AA}^{-1}$ . We calculate rate constants for the field ionization of inert gas atoms as a function of their position above the surface, finding significant enhancement above the protruding surface atoms. We discuss the implications of our results for understanding the mechanism of image formation in the field-ion microscope.

The field-ion microscope (FIM) was the first instrument capable of imaging individual atoms at a surface.<sup>1</sup> Other microscopes with atomic resolution are available today but the FIM still retains some unique features which make it an invaluable tool for surface studies. Current areas of application include measurements of surface diffusion<sup>2</sup> and chemical analysis of surfaces using the atom-probe field-ion microscope.<sup>3</sup> In a FIM, a sharp tip is raised to a high positive voltage so that a large electric field exists near the tip surface. Imaging gas atoms, normally inert gas atoms such as He, are attracted towards the tip by the electric field and are field ionized just above the metal surface. The positively charged ions formed by this process are accelerated by the electric field towards a screen, where they form an image. Normally protruding atoms, such as adatoms or atoms at steps, are imaged, although atomic resolution can also be obtained for some atomically smooth surfaces such as the W (111) surface.

Field ionization is allowed only when the atom is further from the surface than a critical distance because otherwise the atomic-ionization level falls below the Fermi level of the metal and there are no empty states for the electron to tunnel into.<sup>4</sup> As a function of lateral position above the metal surface, the critical distance maps out the critical surface (CS). The tunneling-rate constant is large on the CS and falls rapidly beyond it, so that most of the ionizations occur in a thin crust close to the CS. The image contrast derives from the modulation in the rate of ionization of imaging gas atoms due to the underlying atomic structure of the surface, which could arise from variations in the concentration of gas atoms (the gas concentration mechanism) and/or variations in the tunneling-rate constant (the rate constant mechanism). At low temperatures He atoms are present on the tip surface in large numbers, and it is likely that they are particularly prevalent on top of protruding atoms where the local electric field is largest. However, the potential from a neutral He atom is repulsive<sup>5</sup> and therefore is unlikely that they could enhance local image contrast. The images are not greatly changed by cooling the tip from 80 to 40 K, but at lower temperatures the local image contrast

increases significantly.<sup>6</sup> The simplest explanation of these observations is that at very low temperatures the variations in the gas concentration near the CS are large, so that the gas concentration mechanism is important, but at tip temperatures near 80 K the gas concentration variations are small and the rate constant mechanism is dominant.<sup>6</sup>

A previous calculation of tunneling-rate constants for corrugated model potentials<sup>7</sup> yielded large cross-surface variations, although our work<sup>8</sup> has revealed shortcomings in their study which led to an overestimation of the cross-surface variations by a factor of up to 5. What has been lacking until now are reliable tunneling calculations using potentials which give a realistic description of a metal surface under an applied electric field. In this paper, we report the results of tunneling calculations for the FIM which use potentials obtained from self-consistent pseudopotential calculations of the electron potential for adatom, stepped, and atomically smooth Al (111) surfaces, including a perpendicular applied electric field of  $3 \text{ V \AA}^{-1}$ . These calculations model the actual conditions under which atomic resolution of Al surfaces has been obtained in the FIM.<sup>9</sup> Using these potentials and a JWKB tunneling formalism<sup>10</sup> we calculate the rate constant for an electron to tunnel from an imaging gas atom into the metal surface.

Apart from the image contrast itself, another quantity of interest is the energy distribution of ionized gas atoms arriving at the detector. Measurements of the width of this distribution give values as small as 0.8 eV for imaging of W (110) and (001) surfaces with He atoms and an electric field of  $4.5 \text{ V \AA}^{-1}$ .<sup>1</sup> This narrow energy distribution implies that the region above the CS in which most of the ionization occurs (the ionization zone) is about  $0.8/4.5 \sim 0.2 \text{ \AA}$  wide; however, model potential calculations for flat metal surfaces<sup>11</sup> give considerably larger widths. It is important to give a satisfactory account of the width of the ionization zone, because it is intimately related to the cross-surface variations in the tunneling-rate constant, as both quantities derive from the variation of the rate constant with barrier thickness.

Our calculations were performed using a supercell

technique in which a unit cell, containing a slab of metal and a vacuum region, is repeated throughout space to restore three-dimensional periodicity to the system. For the adatom calculations we used a supercell of length 28.05 Å, which is equivalent to the thickness of 12 atomic layers for the (111) orientation used in this work. Into this cell we placed a slab containing six atomic layers of Al with (111) surfaces. We took translation vectors within the surface plane which were three times the primitive in-plane vectors, so that the surface plane contains nine atoms per unit cell. Finally, an adatom was placed on top of a fcc site on one face of the slab [see Fig. 1(a)] and a second one was placed in an equivalent position on the other face. For the step geometry we used a supercell of length equivalent to 14 atomic layers (32.73 Å) with translation vectors in the surface plane which were six times the primitive in-plane vectors in one direction and equal to a primitive translation vector in the other. To this cell we added a four-layer slab of Al and a stepped surface was created by adding half layers of atoms to each surface of the slab, to give the geometry illustrated in Fig. 1(b).<sup>12</sup> In each case the atomic positions were chosen to be those of truncated bulk Al.

The potentials and wave functions were expanded in a plane-wave basis set containing all waves up to 6 Ry in energy.<sup>13</sup> Brillouin-zone integrations were performed by

$$R = A^2 \nu \int_{\phi=0}^{\phi=2\pi} \int_{\theta=0}^{\theta=\pi/2} \exp \left[ -2^{3/2} \int_{r_0(\theta,\phi)}^{r_1(\theta,\phi)} [V(r,\theta,\phi) - E]^{1/2} dr \right] \sin\theta d\theta d\phi, \quad (1)$$

where  $r_0(\theta,\phi)$  and  $r_1(\theta,\phi)$  are, respectively, the inner and outer classical turning points along the direction  $(\theta,\phi)$  and  $V(r,\theta,\phi)$  is the total potential felt by the tunneling electron whose energy is  $E$ . (The prefactor  $A^2\nu$  has been set to unity for all the results presented in this paper.) This scheme gives excellent results for the uniform-field

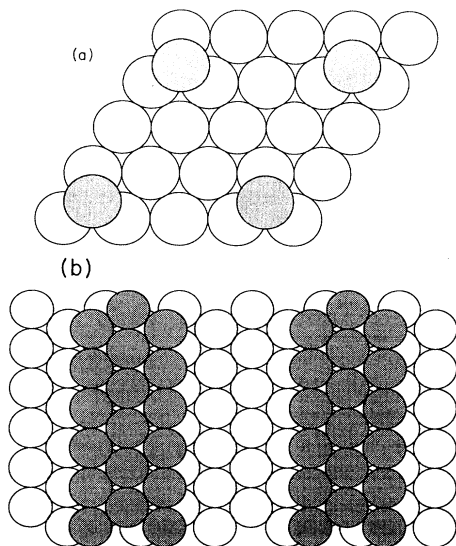


FIG. 1. Top view of (a) the adatom geometry and (b) the stepped surface. The shaded circles represent adatoms and atoms on the upper terrace of the stepped surface while the open circles represent atoms in the layer below.

sampling on regular grids in reciprocal space, containing 50 points for the adatom geometry, 72 points for the step geometry, and 384 points for the atomically smooth (111) surface. We used the Ceperley-Alder form of the local-density approximation for the exchange-correlation potential,<sup>14</sup> and a local pseudopotential to represent the  $\text{Al}^{3+}$  ions,<sup>15</sup> which has been employed successfully in a number of previous calculations. The electric fields were incorporated in the manner described in Ref. 16, i.e., by adding a thin sheet of negative charge in the center of each vacuum region, and adjusting the position of the Fermi level in the metal until charge neutrality was obtained for the supercell as a whole. The resulting potential and charge density in the center of the metal slab are hardly disturbed from the bulk form because the external electric field is fully screened by the buildup of screening charge at the surfaces, which occurs via a depletion of electrons. The charge sheet was chosen to have a Gaussian profile of width 0.529 Å to suppress oscillations in the potential arising from truncation of the basis set.

For our tunneling calculations we used the three-dimensional JWKB formalism of Haydock and Kingham,<sup>10</sup> in which the tunneling-rate constant is given by a summation of one-dimensional contributions from infinitesimal solid angles:

ionization of hydrogenic atoms.<sup>10,17</sup> To evaluate the integrals in Eq. (1), the tunneling potential was stored on a fine grid and a three-dimensional interpolation scheme used to evaluate the integrand at desired points in space. We consider tunneling from atoms over a large range of distances from the surface, and for some of the adatom calculations (but not the step calculations) this requires the extrapolation of the linear portion of the potential, which arises from the applied electric field, out into the vacuum region beyond the position at which we place the negative charge sheet.

To form the total potential we add the potential from the imaging gas atom to that arising from the metal surface and applied field. As discussed elsewhere,<sup>11</sup> the self-consistent potential for an isolated inert gas atom is well represented by a  $-1/4\pi\epsilon_0 r$  potential at, and outside of, the classical turning point, which is the distance from the nucleus at which the potential is equal to the first ionization energy of the atom. We use the experimental values of the first ionization energies of He and Ne (24.5 and 21.5 eV, respectively). Effects arising from the polarization of the imaging gas atoms due to the electric field are expected to be small and have been neglected. The effects of the image potentials of the tunneling electron and the positive ion, which have also been neglected in the present calculations, were discussed in our previous work<sup>11</sup> and we do not believe that their inclusion would make a qualitative difference to our results.

In Fig. 2 we plot the screening charge densities for the adatom and stepped surfaces. The maximum value of the

screening charge density is 0.066 electrons per  $\text{\AA}^3$  above the adatom, 0.034 electrons per  $\text{\AA}^3$  above an atom at the step, and 0.019 electrons per  $\text{\AA}^3$  above an atom in the flat Al (111) surface. Because of the large amount of screening charge above the protruding atoms, the electric-field lines tend to converge on them, which reduces the width of the tunneling barrier in these regions.

In the upper parts of Figs. 2(a) and 2(b) we plot the tunneling-rate constants calculated from Eq. (1) for a He atom on the CS, normalized to the corresponding value for the atomically smooth Al (111) surface above an atom. The ratio of the tunneling-rate constant on top of the adatom to that above an atom in the atomically

smooth Al (111) surface is 7.2. (The plot for Ne atoms is very similar in shape to that for He, and for Ne the tunneling-rate constant on the CS above the adatom is also 7.2 times the corresponding value for the atomically smooth surface.) The rate constant falls rapidly as the gas atom is moved away from the adatom (while remaining on the CS); falling to half its peak value at a distance of 1.85  $\text{\AA}$ . For the stepped surface the variations in the rate constant are not as large, with the ratio of the maximum rate constant for the stepped surface to the corresponding value for the atomically smooth surface being 4.9 (the corresponding ratio for imaging with Ne atoms is 4.0). For the stepped surface the maximum in the rate constant occurs above the center of the terrace, and not above the atoms at the step edges, which is an effect due to the very narrow terrace width. Also note that the rate constant drops slightly below the value for the atomically smooth surface between the adatoms and above the center portion of the lower terrace of the stepped surface. This is also an effect of the short repeat distances within the surface plane.

The minimum cross-surface variation in the rate constant required for atomic resolution has been estimated to be a little less than a factor of 2,<sup>6</sup> although the actual contrast achieved in experiments is probably at least a factor of 10.<sup>3</sup> The cross-surface variations that we have found of a little more than 7 for the adatom geometry are therefore comparable with the experimental estimates and are undoubtedly sufficient to give atomic resolution. Our calculations for atomically smooth Al (111) and (110) surfaces,<sup>16</sup> and for corrugated model potentials,<sup>8</sup> show that the cross-surface variations in the rate constant are an increasing function of the applied electric field. In addition, we have calculated the corrugation of the surface potential for Ir, Au, Pt, and Pb surfaces using a first-principles pseudopotential technique but without an applied field: a typical result is that for the Ir (111) surface the corrugation of the potential at the Fermi energy is 0.4  $\text{\AA}$ , which is twice the value for the Al (111) surface. These results indicate that cross-surface variations in the rate constant considerably larger than a factor of 10 would be obtained for He imaging of, for instance, an Ir adatom at the best-image field of 4.5  $\text{V \AA}^{-1}$ .

We now turn our attention to the variation of the tunneling-rate constant with the distance of the imaging gas atom from the surface. Above the atomically smooth Al (111) surface, the full width at half maximum (FWHM) of the peak in the tunneling-rate constant is calculated to be 0.63  $\text{\AA}$  for imaging with He and a field of 3  $\text{V \AA}^{-1}$ , while for the position above the adatom it is 0.3  $\text{\AA}$ . The width of the peak in the tunneling-rate constant is therefore a strongly decreasing function of the corrugation of the surface potential.<sup>18</sup> These results also imply that the width of the ionization zone should depend significantly on the nature of the site at which the ions are produced, a result which has recently been confirmed by experimental investigations on tungsten surfaces. Unfortunately, we are not aware of any measurements of the energy distribution of ions for Al samples to compare our results with. As discussed above, the surface corrugations for metals such as Ir are considerably larger than

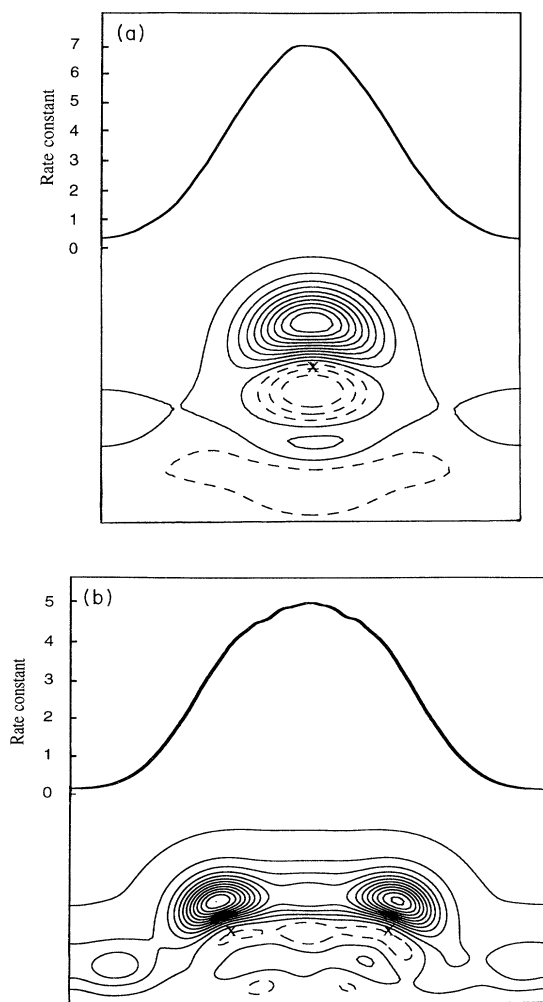


FIG. 2. Screening charge density for (a) the adatom geometry in the plane perpendicular to the surface which passes through the nearest-neighbor adatoms, and (b) the stepped surface in a plane perpendicular to both the surface and the step edges. Solid lines indicate positive screening charge and dashed lines indicate negative screening charge. The positions of the nuclei of the adatom and the atoms at the step edges are denoted by crosses. In the upper portion of the figures the corresponding tunneling-rate constants for He atoms on the critical surface are plotted, normalized to the corresponding values for the atomically smooth Al (111) surface above an atom.

for Al, which would therefore give narrower ionization zone widths, in accord with experiment.

In conclusion, we have used a self-consistent pseudopotential technique to calculate the electron potential outside of Al surfaces with a large applied electric field. We have performed calculations for adatom, stepped, and atomically smooth Al (111) surfaces with an applied electric field of  $3 \text{ V \AA}^{-1}$ , which models the conditions under which FIM images of Al with atomic resolution have been obtained.<sup>9</sup> Tunneling calculations for the FIM using these potentials show that the rate constants for the ionization of He and Ne atoms are significantly enhanced above the protruding atoms because the thickness of the

barrier to tunneling is reduced. An enhancement factor of a little greater than 7 was found for the adatom geometry. The width of the ionization zone is predicted to be significantly reduced by large corrugations of the surface potential. Our results indicate that the atomic resolution of the FIM under normal operating conditions at 80 K can largely be accounted for by cross-surface variations in the rate constant for ionization of the imaging inert gas atoms.

This work was supported by the Science and Engineering Research Council (UK). S.C.L. thanks the Croucher Foundation for financial support.

<sup>1</sup>E. W. Müller and T. T. Tsong, *Field Ion Microscopy: Principles and Applications* (Elsevier, New York, 1969).

<sup>2</sup>G. L. Kellogg, *Phys. Rev. Lett.* **70**, 1631 (1993); S. C. Wang and G. Ehrlich, *ibid.* **70**, 41 (1993); **67**, 2509 (1991); G. L. Kellogg and P. J. Feibelman, *ibid.* **64**, 3143 (1990); C. Chen and T. T. Tsong, *ibid.* **64**, 3147 (1993); S. C. Wang and G. Ehrlich, *ibid.* **62**, 2297 (1989).

<sup>3</sup>T. T. Tsong, *Atom-Probe Field Ion Microscopy* (Cambridge University Press, Cambridge, England, 1990).

<sup>4</sup>M. G. Inghram and R. Gomer, *J. Chem. Phys.* **22**, 1279 (1954).

<sup>5</sup>J. E. Inglesfield and J. B. Pendry, *Philos. Mag.* **34**, 205 (1976).

<sup>6</sup>R. G. Forbes, *J. Phys. D* **18**, 973 (1985).

<sup>7</sup>H. H. Homeier and D. R. Kingham, *J. Phys. D* **16**, L115 (1983).

<sup>8</sup>S. C. Lam and R. J. Needs, *J. Phys. Condens. Matter* **5**, 1195 (1993).

<sup>9</sup>E. D. Boyes and M. J. Southon, *Vacuum* **22**, 447 (1972); W. Zingg and H. Warlimont, *Phys. Status Solidi* **45**, 117 (1978); T. Abe, K. Miyazaki, and K. I. Hirano, *Acta Metall.* **30**, 357 (1982); R. Morgan, *J. Mater. Sci.* **7**, 361 (1972).

<sup>10</sup>R. Haydock and D. R. Kingham, *Surf. Sci.* **103**, 239 (1981).

<sup>11</sup>S. C. Lam and R. J. Needs, *Surf. Sci.* **271**, 376 (1992).

<sup>12</sup>We have also performed calculations for the stepped geometry with the same supercell but containing a six-layer slab of Al; however, the results were not significantly different from the four-layer slab results quoted in this paper.

<sup>13</sup>Calculations for the atomically flat Al (111) surface with a 9-Ry cutoff were also performed, but the resulting tunneling-rate constants were almost unchanged.

<sup>14</sup>D. M. Ceperley and B. J. Alder, *Phys. Rev. Lett.* **45**, 566 (1980), as parametrized by J. P. Perdew and A. Zunger, *Phys. Rev. B* **23**, 5048 (1981).

<sup>15</sup>L. Goodwin, R. J. Needs, and V. Heine, *J. Phys. Condens. Matter* **2**, 351 (1989).

<sup>16</sup>S. C. Lam and R. J. Needs, *Surf. Sci.* **277**, 173 (1992).

<sup>17</sup>S. C. Lam and R. J. Needs, *Surf. Sci.* **277**, 359 (1992).

<sup>18</sup>This conclusion is further supported by the results of tunneling calculations for corrugated model potentials reported in Ref. 8.

<sup>19</sup>N. Ernst, G. Bozdech, H. Schmidt, W. A. Schmidt, and G. L. Larkins, *Appl. Surf. Sci.* **67**, 111 (1993).

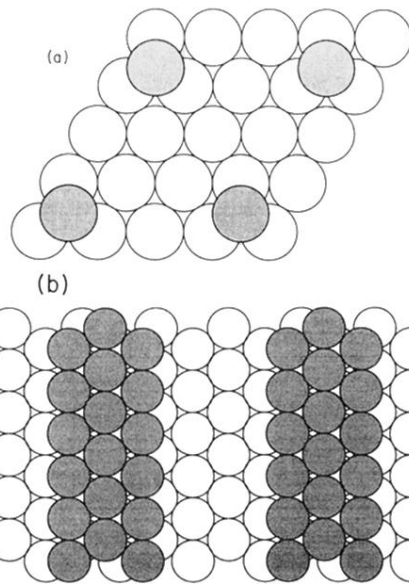


FIG. 1. Top view of (a) the adatom geometry and (b) the stepped surface. The shaded circles represent adatoms and atoms on the upper terrace of the stepped surface while the open circles represent atoms in the layer below.